Catalysis Today 147S (2009) S81–S86

Contents lists available at ScienceDirect

Catalysis Today

journal homepage: www.elsevier.com/locate/cattod

Design of Pt–Sn catalysts on mesoporous titania films for microreactor application

Z.R. Ismagilov [a,*], E.V. Matus [a], A.M. Yakutova [a], L.N. Protasova [a,b], I.Z. Ismagilov [a], M.A. Kerzhentsev [a], E.V. Rebrov [b], J.C. Schouten [b]

[a] *Boreskov Institute of Catalysis, Novosibirsk, 630090, Russia*
[b] *Eindhoven University of Technology, Eindhoven, P.O. Box 513, 5600 MB, The Netherlands*

ARTICLE INFO

Article history:
Available online 4 August 2009

Keywords:
Mixed-metal clusters
Pt–Sn
Mesoporous titania
Citral hydrogenation

ABSTRACT

A new generation of nanostructured Pt–Sn/TiO_2 catalytic thin films has been developed by deposition of Pt–Sn mixed-metal precursors from organic solvents on mesoporous TiO_2/Ti films with a thickness of 200–300 nm. The titania sol was obtained by templating a TiO_2 precursor with Pluronic F127 surfactant. The films were prepared on Ti substrates by spin-coating. The influence of the F127/Ti ratio in the range between 0.006 and 0.050, the pH of the titania sol between 1.5 and 2.0, and the aging time between 8 and 240 h on the morphology and porous structure of titania films was investigated. A TiO_2 film with the highest degree of the long-order structure was obtained at a surfactant/Ti molar ratio of 0.009, a pH of 1.5, and an aging time of 24 h. This film has a hexagonal pore structure with a mean pore size of 3.5 nm and a porosity of 25%. A powder titania support with a similar chemical composition and morphology was also produced and used for optimization of an active component deposition. The Pt–Sn carbonyl $[Pt_3(CO)_3(SnCl_3)_2(SnCl_2{\cdot}H_2O)]_n^{-2n}$ clusters were synthesized separately from monometallic precursors. They were loaded onto the TiO_2 supports by impregnation or adsorption. The adsorption of the Pt–Sn precursor for 24 h from an ethanol solution with concentrations of Pt and Sn of 2.0 and 1.2 mg/ml, respectively, followed by a vacuum treatment at 463 K, resulted in Pt–Sn nanoparticles embedded in the mesoporous titania network. An average size of bimetallic nanoparticles was 1.5–2 nm with a narrow particle size distribution. A reaction rate in terms of TOF between 0.2 and 3.3 min^{-1} was observed in the hydrogenation of citral over the Pt–Sn/TiO_2 catalysts. The selectivity to the unsaturated alcohols was as high as 90% at a citral conversion above 95%.

1. Introduction

Multiphase reactions can be performed in structured reactors, which improve heat and mass transfer, allow isothermal operation and provide narrow residence time distribution [1]. There are several application areas, where catalytic microreactors have evident advantages over traditional reactors, among which small-scale energy generation, fuel processing [1,2], and synthesis of fine chemicals [3]. The efficient use of catalytic reactors requires shaping of the catalyst by deposition of thin catalytic films on the inner walls of the reactor channels. Inorganic mesoporous thin films have attracted considerable attention because of their large surface areas and narrow pore size distribution, which make them attractive candidates for catalyst supports [4–6].

The efficiency of catalytic microreactors strongly depends on deposition of uniform catalytic coatings with good adhesion, high surface area, good dispersion of the active component, and high stability. Depending on the geometry of the channel and substrate type, different methods for deposition of thin catalytic porous layers with uniform thickness have been developed, among others, anodic oxidation [7], vapor deposition techniques (ALD, CVD) [8] and sol–gel methods (spin-coating, dip-coating) [4,9].

This study is devoted to the development of mesoporous titania supported novel Pt–Sn bimetallic nanostructured catalysts derived from mixed-metal precursors with desirable stoichiometry between the metals. The unique characteristics of mesostructured titania, namely high surface area, high concentration of hydroxyl groups combined with narrow pore size distribution prevent metal sintering after catalyst deposition. This approach allows a control both of the metal ratio and the loading of the support with the bimetallic nanoparticles. These nanoparticles demonstrate a superior performance in the selective hydrogenation of unsaturated aldehydes to the corresponding unsaturated alcohols (UA) as compared to the "crude" catalysts fabricated via impregnation-reduction methods.

---

[*] Corresponding author at: Boreskov Institute of Catalysis SB RAS, Prospekt Akademika Lavrentieva, 5, 630090 Novosibirsk, Russian Federation.
Tel./Fax: +7 383 330 62 19.
E-mail address: zri@catalysis.ru (Z.R. Ismagilov).

0920-5861/$ – see front matter © 2009 Elsevier B.V. All rights reserved.
doi:10.1016/j.cattod.2009.07.046

2. Experimental

2.1. Synthesis of Pt–Sn mixed-metal cluster precursor

The Pt–Sn bimetallic clusters were synthesized by a procedure adopted from Ref. [10]. An aqueous $H_2PtCl_6 \cdot 6H_2O$ (37.5 wt.% Pt, Aurat) solution with a Pt concentration of 2–10 mg/ml was carbonylated at 297 K for 16 h to yield the $H_2[Pt_3(CO)_6]_{10}$ cluster, which converts under CO atmosphere in an organic solvent giving the Chini anion: $[Pt_3(CO)_6]_n^{2-}$, where $n = 5$ or 6. In this study, acetone, ethanol, or tetrahydrofuran (THF) were used as a solvent. In the next step, a desired amount of HCl and $SnCl_2 \cdot 2H_2O$ (98 wt.%, Soyuzkhimprom) was added to the Chini anion solution under CO atmosphere. After a reaction time of 2 h, $[Pt_3(CO)_3(SnCl_3)_2(SnCl_2 \cdot H_2O)]_n^{-2n}$ mixed-metal clusters were formed. They were isolated by addition of a tetraethyl ammonium chloride solution.

2.2. Preparation of mesoporous titania supports

Titanium substrates (99.99+ wt.% Ti) of 10 × 10 mm^2 with a thickness of 500 μm were cleaned and pretreated as described elsewhere [4]. Immediately prior to the synthesis, the titania layer formed during pretreatment procedures was made super hydrophilic (concentration of surface OH groups >15/nm^2) by UV treatment for 2 h to encourage better adhesion of the titania film to the substrate.

A titania precursor sol of composition 1 $Ti(O\text{-}iPr)_4$:0.006–0.050 F127:40 ethanol:1.3 H_2O:0.1 trifluoroacetic acid was synthesized. The solution was prepared by dissolving the templating agent (Pluronic F127, $EO_xPO_yEO_x$, EO = ethylene oxide, PO = propylene oxide, $x = 100$, $y = 65$, BASF) in absolute ethanol, followed by the addition of water and trifluoroacetic acid. Titanium (IV) isopropoxide ($Ti(O\text{-}iPr)_4$, 99.99%, Fluka) was added dropwise to the rapidly stirred solution, and the resulting mixture was left to age under stirring for different time intervals (8–240 h) at room temperature.

Then, a desired amount of the solution was added onto the surface of a titanium substrate and the solvent was evaporated by spin-coating at 1500 rpm for 30 s at a relative humidity of 80%. The samples were dried at room temperature and then calcined at 573 K for 4 h under a residual pressure of 10 mbar with a heating rate of 1 K/min to remove the surfactant [11].

The mesoporous titania powders were prepared by sol–gel method using the same precursors and aging protocol with the only difference that nitric acid was used instead of trifluoroacetic acid. The pH during hydrolysis was varied between 1.5 and 2.0, and the Pluronic F127/($Ti(O\text{-}iPr)_4$ molar ratio between 0.005 and 0.009. The resulting solution was stirred for 24 h. The solvent was evaporated under an IR-lamp for 3 h, followed by a treatment in a desiccator at 373 K for 1 h and calcination at 823 K for 4 h. The samples represent a white powder.

2.3. Preparation of supported Pt–Sn/TiO_2 catalysts

The $[Pt_3(CO)_3(SnCl_3)_2(SnCl_2 \cdot H_2O)]_n^{-2n}$ solution was deposited onto the titania support by impregnation or adsorption for time intervals between 24 and 96 h.

For the powder TiO_2, the loading from 20 and 100 ml of solution of the Pt–Sn precursor for 1 g of TiO_2 was used. For the preparation of Pt–Sn catalysts on titania films, 50 titanium plates with TiO_2 films were fixed in a holder and then immersed in 150 ml of an ethanol solution of the Pt–Sn mixed-metal cluster for time intervals between 24 and 96 h. After adsorption, the impregnated TiO_2 materials were washed by a solvent, dried in vacuum and subsequently heated in vacuum at 463 K.

For comparison, the Pt–Sn/TiO_2 powered samples were also prepared by co-impregnation using $H_2PtCl_6 \cdot 6H_2O$ and $SnCl_2 \cdot 2H_2O$ as metals precursors.

The samples are referred to according to their synthesis procedure: the first letter denotes loading mode: "A" and "I" stand for adsorption and impregnation, respectively. The second letter corresponds to the solvent used: "A", "E", and "T" stand for acetone, ethanol, and THF, respectively. The combination of letters at the third place denotes the type of activation treatment: "V" means heated under vacuum at 463 K, "OR" means oxidized (calcined) in O_2 at 673 K and subsequently reduced in a 30 vol.% H_2/Ar flow at 673 K. The number at the end stands for the platinum concentration in the initial solution (mg/ml).

2.4. Characterization of mesoporous titania and Pt–Sn/TiO_2 catalysts

The chemical composition of the prepared catalysts was determined by X-ray fluorescence spectroscopy using a VRA-30 analyzer with a Cr anode of an X-ray tube. The phase composition was determined by X-ray diffraction in the range of 0.5–4° 2-theta.

The morphology of the TiO_2, the average Pt–Sn nanoparticle size and particle size distribution (PSD) were determined with a high-resolution JEOL JEM-2010 transition electron microscope operating at 200 kV with a structural resolution of 0.14 nm. The samples were deposited on perforated carbon supports attached to the copper grids. The local elemental analysis of the samples was carried out by an Energy Dispersive X-ray Analysis (EDX) method using an EDAX spectrometer equipped with a Si (Li) detector with a resolution of 130 eV.

The BET surface area and the porosity of the powder supports and catalysts were determined on a Micromeritics ASAP 2400 instrument using nitrogen adsorption at 77 K. The mesopore volume, mesopore surface area, and the pore size distribution, of the TiO_2 films were determined by ellipsometric porosimetry. The details of the method are described elsewhere [12].

2.5. Catalytic activity test

Two types of catalytic tests were performed: (i) either fifty Pt–Sn/TiO_2/Ti plates were inserted in a holder at a 2 mm separation, or (ii) catalyst pellets with a particle size of 100–200 μm were fixed in a basket. The holder with the catalyst was placed in an autoclave reactor with a total volume of 270 ml. The catalysts were reduced at 523 K under 12 bar of H_2 pressure for 12 h. Then the reactor was cooled to room temperature. The hydrogenation of a 0.01 M citral solution in 2-propanol was performed at 343 K and 12 bar H_2 with the plate holder rotating at 1500 rpm. Analysis was performed by introducing aliquots at established time intervals into a Varian CP-3800 GC equipped with a CP-Sil 5 CB capillary column via an automatic rapid on-line sampler-injector system (ROLSI^{TM}). The main reaction products were nerol, geraniol, citrononellal, citronellol and 3,7-dimethyl-1-octanol. The carbon balance was closed within 99% in all experiments.

3. Results and discussion

3.1. Synthesis of mesoporous TiO_2 materials

The samples of TiO_2 powder were prepared via sol–gel route at several different surfactant to titanium ratios 0.005–0.009 and pH of 1.5, 1.8, 2.0. The samples exhibit a IV type isoterms with a hysteresis loop at a N_2 partial pressure of 0.8 which is associated with textural mesoporosity [6,7]. The average pore size is 3.5–6.8 nm and the total pore volume is 0.04–0.16 cm^3/g. The specific surface area increases from 20 to 90 m^2/g with rising F127/Ti molar ratio from 0.005 to 0.008 at a given pH. These data are close to

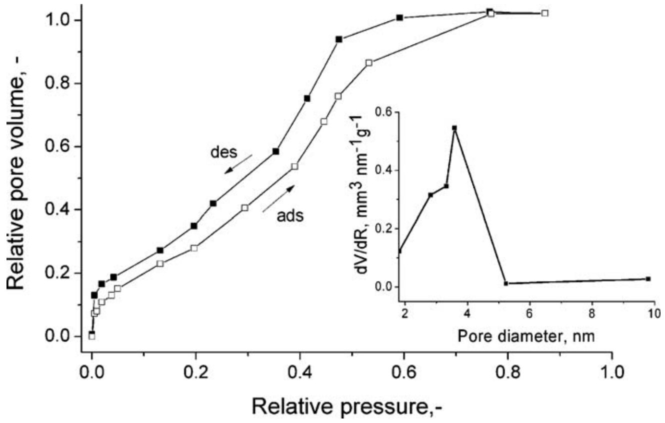

Fig. 1. The ethanol adsorption–desorption isotherms at 287 K and the pore size distribution for the mesoporous titania film. Synthesis conditions: F127/Ti ratio: 0.009, pH: 1.5, aging time: 24 h.

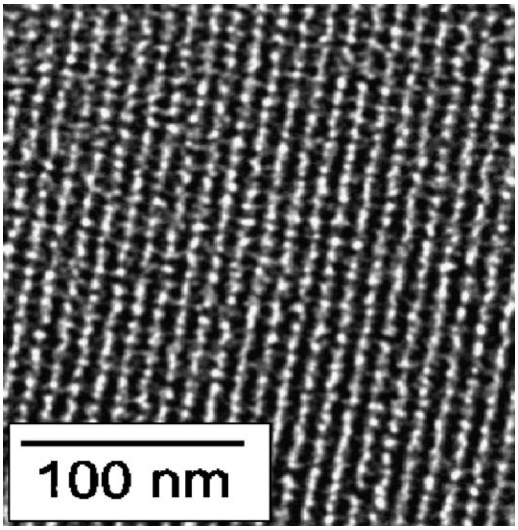

Fig. 2. TEM image of the mesoporous titania film taken after storage in air at room temperature for 2 months. Synthesis conditions are the same as those in Fig. 1.

those reported in literature [13,14]. It seems that the low porosity of the prepared TiO_2 is connected with a high calcination temperature and a long duration of the calcination required for the surfactant removal. Anatase was the only phase in the samples based on the XRD analysis data.

The TiO_2 coatings were synthesized on titania substrates by evaporation-induced self assembly (EISA) assisted sol–gel method at variation of surfactant to titanium ratios, pH and aging time. Typical ethanol adsorption–desorption isoterms are shown in Fig. 1. The type IV isotherm with a H1 hysteresis loop at ethanol partial pressure of 0.3–0.5 indicates to the framework-confined mesopores [13,15]. The increase of the aging time leads to increasing of the sol viscosity, thereby enlarging the thickness of the resulting film. For the titanium films, hexagonal mesostructure was confirmed by LA-XRD and TEM in the whole range of the compositions studied. A typical example of the mesoporous structure is shown in Fig. 2. As the F127/Ti molar ratio increases from 6×10^{-3} to 9×10^{-3}, the unit cell size decreases from 9.3 to 7.0 nm with the substantial increase in open porosity from 14 to 25%.

The surfactant was completely removed even at mild conditions as confirmed by the absence of the absorption bands at 1110, 2850 and 2930 cm^{-1} in the FTIR spectra of the mesoporous titania films. After calcination, the film thickness was reduced to 200 nm, which is almost a half of that in the as-synthesized samples.

3.2. Preparation of Pt–Sn/TiO_2 supported catalysts

To optimize the conditions of Pt–Sn cluster loading onto TiO_2, several synthesis parameters have been systematically varied, among them (i) solvent type (acetone, ethanol, or THF), (ii) concentration of the precursor solution (2.0, 10 mgPt/ml; 1.2, 6.0 mgSn/ml), (iii) the metal precursor to support ratio (20, 100 ml/g), (iv) duration of adsorption (2, 24 h), and (v) type of the activation treatment (calcined in O_2 at 673 K for 4 h and subsequently reduced in a 30 vol.% H_2/Ar flow at 673 K for 2 h, or in vacuum at 463 K for 2 h). In addition, the influence of the nature of the bimetallic precursor (carbonyl mixed-metal cluster or inorganic metal salts) was studied. Table 1 presents the effect of synthesis conditions on the properties of Pt–Sn/TiO_2 powder catalysts.

The metal loading in supported bimetallic catalysts prepared by adsorption of the bimetallic carbonyl precursor depends on the solvent type and increases in a sequence: acetone < ethanol < THF. This seems to be related to a difference in solubility of the precursor in these solvents. Fig. 3 reports TEM images of AE-OR-2 and AT-OR-2 catalysts showing numerous particles 1–3 nm of size. Fig. 4 shows the image of one of these

Table 1
Synthesis conditions and properties of powered Pt–Sn/TiO_2 catalysts.

Sample name	Synthesis conditions				Catalyst composition			Average particle size, nm
	Concentration in solution, mg/ml		Duration of loading, h	Thermal treatment[a]	Pt, wt.%	Sn, wt.%	Pt/Sn molar ratio	
	Pt	Sn						
Mixed-metal cluster precursor								
AA-OR-2	2	1.2	24	OR	0.05	0.04	1.2	0.7
AE-OR-2	2	1.2	24	OR	0.61	0.25	1.5	1.1
AT-OR-2	2	1.2	24	OR	4.04	1.75	1.5	2.2
AE-OR-10	10	6	24	OR	3.55	2.80	0.8	3.2
IE-OR-2	2	1.2	72	OR	3.46	1.33	1.6	n.d.
AE-V-2	2	1.2	24	V	0.61	0.25	1.5	1.5
IT-OR-2	2	1.2	72	OR	3.67	2.29	1.0	1.6
Inorganic metal salt precursor								
IE-OR-33	33	20	0.25	OR	2.16	0.95	1.4	1.8
IA-OR-33	33	20	0.25	OR	2.16	1.05	1.3	1.7

n.d.—not determined.

[a] OR—oxidized (calcined) in O_2 at 673 K for 4 h and subsequently reduced in a 30 vol.% H_2/Ar flow at 673 K for 2 h; V—heated under vacuum at 463 K for 2 h.

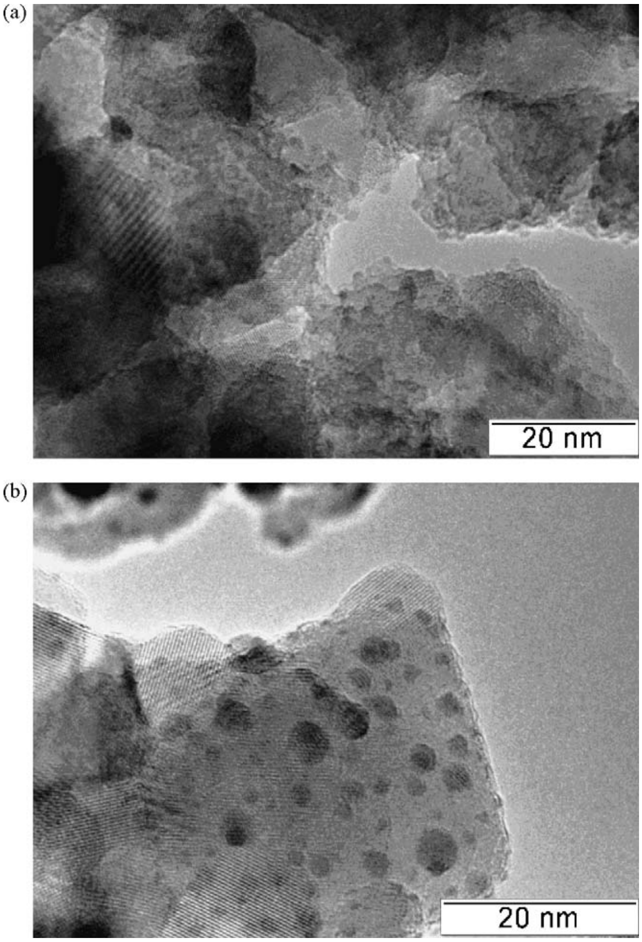

Fig. 3. TEM images of Pt–Sn/TiO_2 catalysts with different metal loadings: (a) 0.61 wt.% Pt, 0.25 wt.% Sn (AE-OR-2, Table 1); (b) 4.04 wt.% Pt, 1.75 wt.% Sn (AT-OR-2, Table 1).

metal particles. According to the Fourier pattern, this particle has a crystalline structure with lattice spacings of 2.14, 2.32, 4.29 Å. This structure can be assigned to a Pt_3Sn alloy with lattice spacings of $d_{2\,0\,0} = 2.0015$ Å, $d_{1\,1\,1} = 2.3107$ Å, and $d_{1\,0\,0} = 4.001$ Å. The increase of metals content from 0.1 to 0.6 to ca. 4 wt.% Pt resulted in an increase of the average particle size from 1 to 2 nm. At the same time, the PSD pattern changed from mono- to bi-modal (Fig. 5).

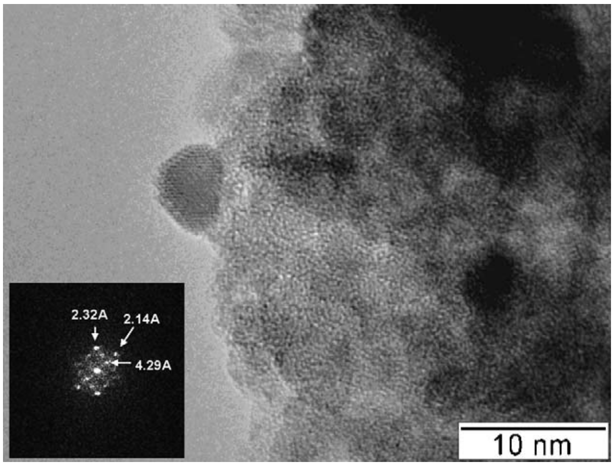

Fig. 4. TEM image of AT-OR-2 sample. Inset: Fourier pattern and lattice spacings.

The increase of the mixed-metal cluster concentration in the solution (from 2 to 10 mgPt/ml) leads to a proportional rise of the metal loading (from 0.6 to 3.5 wt.% Pt), average particle size (from 1.5 to 3.2 nm) and to a wider PSD in the Pt–Sn/TiO_2 samples. For the both samples, PSD has a monomodal type. It is necessary to note that an increase of the metal precursor to support ratio and the duration of adsorption step also leads to higher metal loadings in the catalysts. When a mixed-metal cluster precursor is deposited by impregnation it allows increasing the metal loading in the catalysts (sample IE-OR-2 and IT-OR-2, Table 1).

The crystalline structure of particles was not significantly affected by the mode of thermal treatment. The Pt_3Sn nanoparticles were observed in the sample after treatment in vacuum (Fig. 6). A vacuum catalyst activation procedure also resulted in a narrow PSD in comparison with that after reduction by hydrogen (compare Figs. 7 and 5a). The range of obtained particle sizes is 0.5–5.1 and 0.5–2.9 nm, respectively for oxidative and vacuum treatments.

The mixed-metal cluster precursor provided a more uniform metal particle size distribution as compared with inorganic metal salt precursors at the practically same average particle size. In particular, for catalysts prepared by co-impregnation from H_2PtCl_6 and $SnCl_2$ precursors, large nanoparticles of 20 nm were also obtained while the average particle size was ca. 2 nm. In these catalysts in addition to Pt_3Sn nanoparticles the Pt and Pt_2Sn_3 particles were observed.

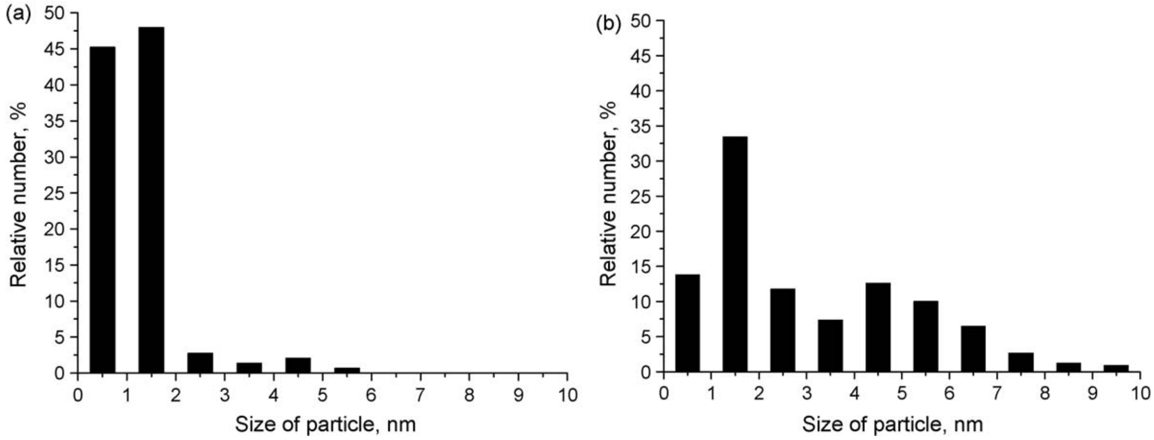

Fig. 5. Size distribution of Pt–Sn particles in the Pt–Sn/TiO_2 catalysts with different metal loading: (a) 0.61 wt.% Pt, 0.25 wt.% Sn (AE-OR-2, Table 1); (b) 4.04 wt.% Pt, 1.75 wt.% Sn (AT-OR-2, Table 1).

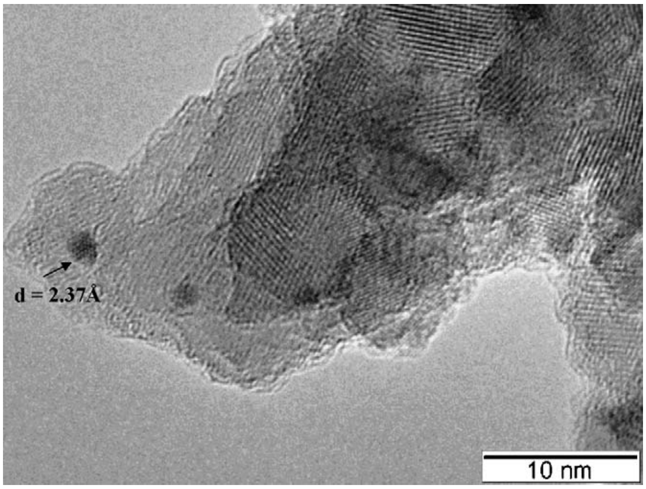

Fig. 6. TEM image of AE-V-2 sample after vacuum treatment at 463 K.

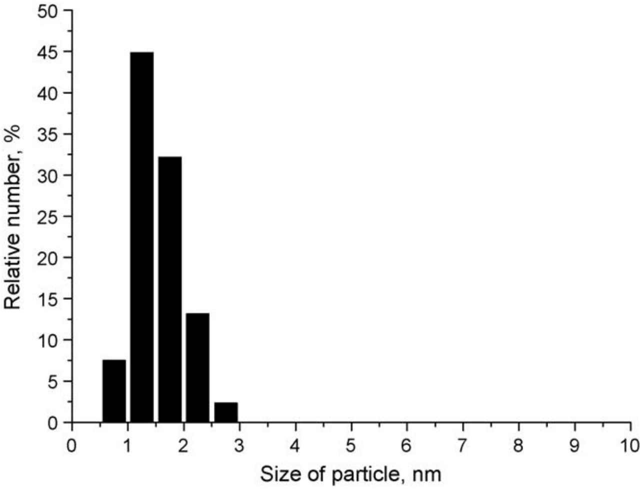

Fig. 7. Size distribution of Pt–Sn particles in the Pt–Sn/TiO_2 catalyst after vacuum treatment at 463 K (AE-V-2, Table 1).

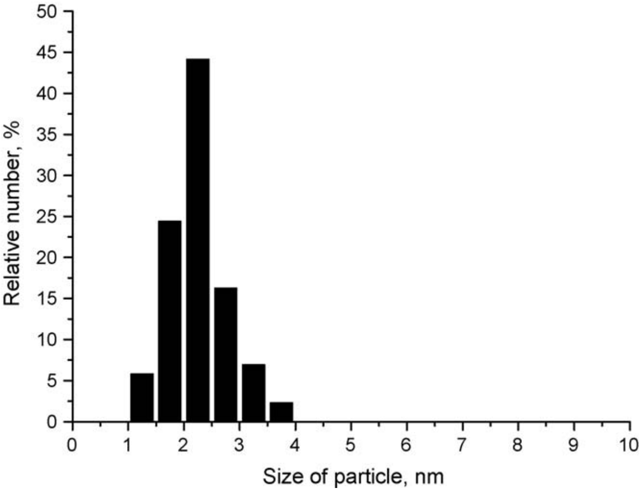

Fig. 8. Size distribution of Pt–Sn particles in the Pt–Sn/TiO_2 catalytic film prepared by adsorption of Pt–Sn–CO anion complex onto TiO_2 film during 24 h.

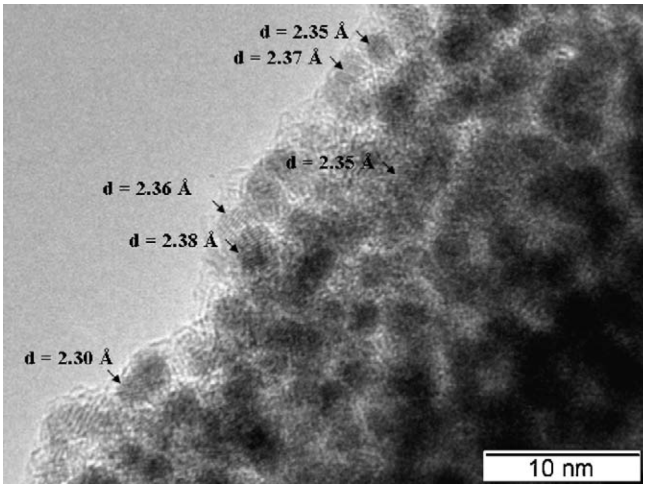

Fig. 9. TEM image of Pt–Sn/TiO_2 catalytic film prepared by adsorption of Pt–Sn–CO anion complex onto TiO_2 film during 24 h.

The prolonged adsorption (96 h) of the mixed-metal cluster precursor from the ethanol solution onto TiO_2 films leads to a decrease of the porosity from 25 to 8% and the average pore size from 3.5 to 1.8 nm. The Pt–Sn/TiO_2 film had a smaller mean pore size as compared to the pure titania support due to a partial pore blockage by the metal nanoparticles. Using TEM, the average Pt–Sn particle size was found to be 9.1 nm. Hence the pore size of the titania film (about 2 nm) is smaller than the average Pt–Sn particle size.

As noted above, for powdered Pt–Sn/TiO_2 catalysts the average particle size is about 1–3 nm. The larger particle size for Pt–Sn/TiO_2

Table 2
Activity and selectivity of powered Pt–Sn/TiO_2 catalysts.

Sample	Initial TOF, min^{-1}	Product selectivity at the 96–98% citral conversion, %			
		Nerol and Geraniol	Citronellal	Citronellol	3,7-Dimethyl-1-octanol
Mixed-metal cluster precursor					
Pt/TiO_2	5.6	3	11	21	65
AA-OR-2	n.d.	n.d.	n.d.	n.d.	n.d.
AE-OR-2	0.06	65	28	6	1
AT-OR-2	0.20	82	7	10	1
AE-OR-10	0.54	90	6	4	0
IE-OR-2	0.35	80	4	16	0
AE-V-2	0.18	39	35	26	0
IT-OR-2	0.14	90	4	6	0
Inorganic metal salt precursor					
IE-OR-33	3.3	85	0	15	0
IA-OR-33	0.32	70	4	17	9

n.d.—not determined.

film is probably connected with a long time of adsorption step (96 h) during its preparation. Actually the reduction of the duration of the adsorption of carbonyl complex anion onto the TiO_2 film from 96 to 24 h leads to the decrease of an average particle size from 9.1 to 2.3 nm (Fig. 8). Fig. 9 shows the TEM image of Pt–Sn/TiO_2 catalytic coatings prepared by adsorption for 24 h. The lattice spacing of the observed nanoparticles is indicative of the bimetallic composition of particles.

3.3. Activity of Pt–Sn/TiO_2 catalysts

The catalytic activity of the Pt–Sn/TiO_2 catalysts was determined in the hydrogenation of citral employing a 0.01 M solution of citral in 2-propanol at 343 K and 12 bar H_2 (Table 2). The activity of a reference Pt/TiO_2 sample characterized by the initial TOF was found to be 5.6 min^{-1} with the selectivity to unsaturated alcohols of 3%. The addition of tin to the Pt/TiO_2 catalysts resulted in TOF lowering and an increase of the selectivity to UA, which is in agreement with previously reported literature data [16,17].

The Pt–Sn/TiO_2 catalysts prepared using Pt–Sn mixed-metal cluster precursor and oxidation–reduction thermal treatment showed a TOF of 0.1–0.5 min^{-1} and a selectivity to UA of 65–90%. In the beginning of the reaction the selectivity to UA is growing with the increase of citral conversion and then stay at the plateau. Most of the citral was converted into UA, while citronellal, citronellol were formed in small amounts. The fully saturated product (3,7-dimethyl-1-octanol) was only observed at high conversion of citral. The samples after vacuum thermal treatment exhibited a lower selectivity to UA at the same TOF in comparison with the samples after OR thermal treatment. The sample obtained using high concentration of Pt in initial solution (10 mg/ml) showed a very high selectivity to UA (90%) and TOF of 0.54 min^{-1}. A higher activity was demonstrated by Pt–Sn/TiO_2 catalyst (IE-OR-33) prepared using combined impregnation of the inorganic salts as metal precursors. This sample showed a TOF of 3.3 min^{-1} and a selectivity to UA of 85%. It can be supposed that such high TOF value is connected with the peculiarity of the composition of bimetallic particles and electronic state of metals. A similar effect was observed over Rh–Sn/SiO_2 catalysts in citral hydrogenation in [18]. The activity of catalysts prepared by co-impregnation was three-folds higher than that of the catalysts prepared via organometallic route and successive impregnation. This could be attributed to an intimate contact between the metals. A metal–metal interaction plays an essential role in the reaction over bimetallic catalytic systems.

4. Conclusions

Mesoporous titania films with hexagonal pore structure and a thickness of 200–300 nm were successfully prepared on Ti substrates by the sol–gel method using the Pluronic F127 as a template. The morphology and porous structure of titania films were regulated by the variation of the F127/Ti ratio in the range between 0.006 and 0.050, the pH of the titania sol between 1.5 and 2.0, and the aging time between 8 and 240 h. Powder titania supports were also produced by the same manner and used for the optimization of catalyst preparation.

Pt–Sn/TiO_2 catalyst films on the Ti plates and powdered Pt–Sn/TiO_2 catalysts were obtained by loading Pt–Sn carbonyl complex anionic species $[Pt_3(CO)_3(SnCl_3)_2(SnCl_2{\cdot}H_2O)]_n^{-2n}$ onto TiO_2 supports. It was shown that the metal content, mean particle size and mode of PSD in the Pt–Sn/TiO_2 catalysts can be varied by changing conditions of the Pt–Sn carbonyl complex adsorption and the thermal treatment of Pt–Sn/TiO_2 catalysts. The mean diameter of anchored bimetallic nanoparticles decrease from 9.1 to 2.3 nm with a reduction of the adsorption duration from 96 to 24 h.

A reaction rate in terms of TOF between 0.2 and 3.3 min^{-1} was observed in the hydrogenation of citral over the Pt–Sn/TiO_2 catalysts with a selectivity to the UA as high as 90% at a citral conversion above 95%.

Acknowledgements

The authors are thankful to A.V. Ishchenko for the assistance with catalyst characterization by HRTEM and EDX. Financial support of this work in the frame of NWO-RFBR 047.017.028 project is gratefully acknowledged.

References

[1] G. Kolb, V. Hessel, Chem. Eng. J. 98 (2004) 1–38.
[2] I.Z. Ismagilov, E.M. Michurin, O.B. Sukhova, L.T. Tsykoza, E.V. Matus, M.A. Kerzhentsev, Z.R. Ismagilov, A.N. Zagoruiko, E.V. Rebrov, M.H.J.M. de Croon, J.C. Schouten, Chem. Eng. J. 135 (2008) S57–S65.
[3] E.V. Rebrov, A. Berenguer-Murcia, H.E. Skelton, B.F.G. Johnson, A.E.H. Wheatley, J.C. Schouten, Lab Chip 9 (2009) 503–506.
[4] T.S. Glazneva, E.V. Rebrov, J.C. Schouten, E.A. Paukshtis, Z.R. Ismagilov, Thin Solid Films 515 (2007) 6391–6394.
[5] O. Muraza, E.V. Rebrov, T. Khimyak, B.F.G. Johnson, P.J. Kooyman, U. Lafont, M.H.J.M. de Croon, J.C. Schouten, Chem. Eng. J. 135 (2008) S99–S103.
[6] E.V. Rebrov, A. Berenguer-Murcia, B.F.G. Johnson, J.C. Schouten, Catal. Today 138 (2008) 210–215.
[7] I.Z. Ismagilov, R.P. Ekatpure, L.T. Tsykoza, E.V. Matus, E.V. Rebrov, M.H.J.M. de Croon, M.A. Kerzhentsev, J.C. Schouten, Catal. Today 105 (2005) 516–528.
[8] M.T. Janicke, H. Kestenbaum, U. Hagendorf, F. Schüth, M. Fichtner, K. Schubert, J. Catal. 191 (2000) 282–293.
[9] K. Haas-Santo, M. Fichtner, K. Schubert, Appl. Catal. A 220 (2001) 79–92.
[10] N.B. Shitova, Y.D. Perfil'ev, L.Y. Al't, G.G. Savel'eva, Russ. J. Inorg. Chem. 46 (2001) 376–381.
[11] L.N. Protasova, E.V. Rebrov, T.S. Glazneva, A. Berenguer-Murcia, Z.R. Ismagilov, J.C. Schouten, J. Catal. (submitted for publication).
[12] L.N. Protasova, E.V. Rebrov, Z.R. Ismagilov, J.C. Schouten, Micropor. Mesopor. Mater. 123 (2009) 243–252.
[13] T.-D. Nguyen-Phan, M.B. Song, E.J. Kim, E.W. Shin, Micropor. Mesopor. Mater. 119 (2009) 290–298.
[14] M.M. Yusuf, H. Imai, H. Hirashima, J. Sol–Gel Sci. Tech. 28 (2003) 97–104.
[15] T.R. Pauly, Y. Liu, T.J. Pinnavaia, S.J.L. Billinge, T.P. Rieker, J. Am. Chem. Soc. 121 (1999) 8835–8842.
[16] J.C.S. Wu, W.-C. Chen, Appl. Catal. A 289 (2005) 179–185.
[17] A.M. Silva, O.A.A. Santos, M.J. Mendes, E. Jordao, M.A. Fraga, Appl. Catal. A 241 (2003) 155–165.
[18] J.N. Coupé, E. Jordão, M.A. Fraga, M.J. Mendes, Appl. Catal. A 199 (2000) 45–51.